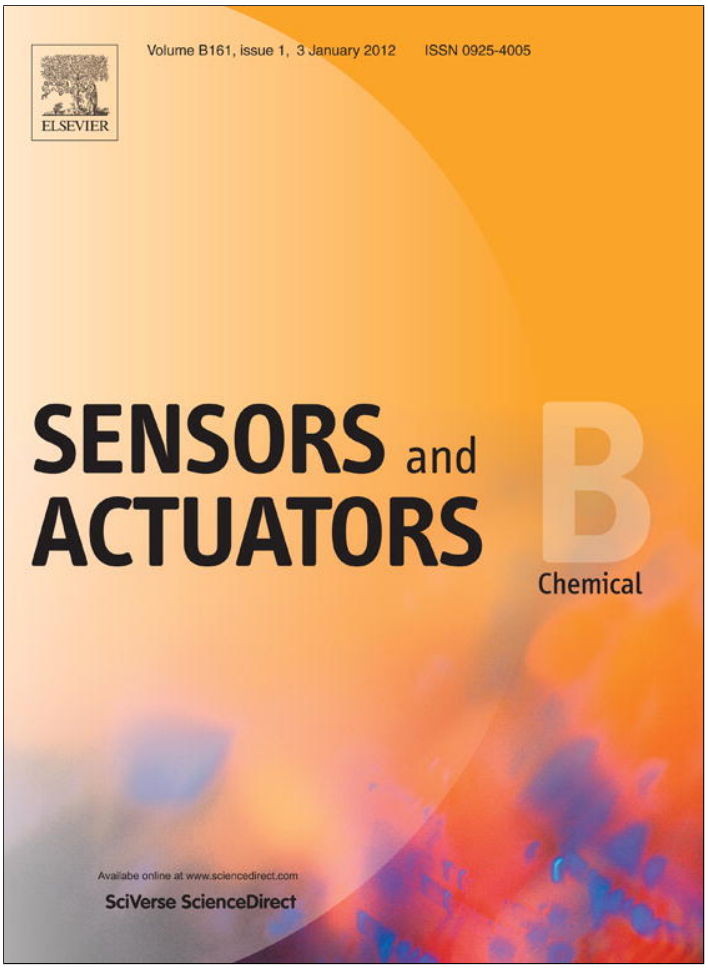

Sensors and Actuators B 161 (2012) 349–358

Contents lists available at SciVerse ScienceDirect

Sensors and Actuators B: Chemical

journal homepage: www.elsevier.com/locate/snb

Inhibitory effect of common microfluidic materials on PCR outcome

Rimantas Kodzius[a,b,*], Kang Xiao[c], Jinbo Wu[d], Xin Yi[d], Xiuqing Gong[d], Ian G. Foulds[b], Weijia Wen[a,d]

[a] KAUST-HKUST Micro/Nanofluidic Joint Laboratory, The Hong Kong University of Science and Technology, Clear Water Bay, Kowloon, Hong Kong
[b] Division of Physical Sciences and Engineering, 4700 King Abdullah University of Science and Technology, Thuwal 23955-6900, Saudi Arabia
[c] Department of Biology, The Hong Kong University of Science and Technology, Clear Water Bay, Kowloon, Hong Kong
[d] Nano Science and Nano Technology Program and Physics Department, The Hong Kong University of Science and Technology, Clear Water Bay, Kowloon, Hong Kong

ARTICLE INFO

Article history:
Received 23 July 2011
Received in revised form 10 October 2011
Accepted 17 October 2011
Available online 25 October 2011

Keywords:
Bovine serum albumin (BSA)
Microfluidics
PCR (polymerase chain reaction)
PCR compatibility
Polymerase
Surface passivation

ABSTRACT

In this study, we established a simple method for evaluating the PCR compatibility of various common materials employed when fabricating microfluidic chips, including silicon, several kinds of silicon oxide, glasses, plastics, wax, and adhesives. Two-temperature PCR was performed with these materials to determine their PCR-inhibitory effect. In most cases, adding bovine serum albumin effectively improved the reaction yield. We also studied the individual PCR components from the standpoint of adsorption. Most of the materials did not inhibit the DNA, although they noticeably interacted with the polymerase. We provide a simple method of performing PCR-compatibility testing of materials using inexpensive instrumentation that is common in molecular biology laboratories. Furthermore, our method is direct, being performed under actual PCR conditions with high temperature. Our results provide an overview of materials that are PCR-friendly for fabricating microfluidic devices. The PCR reaction, without any additives, performed best with pyrex glass, and it performed worst with PMMA or acrylic glue materials.

1. Introduction

Microfluidic chips have a variety of applications in the biological sciences and medicine. In contrast with traditional experimental approaches, microfluidics entails lower sample and reagent consumption, allows faster reactions and enables efficient separation. Additionally microfluidics offers other advantages accruing from the fluids' various distinct behaviors, such as energy dissipation, fluidic resistance, laminar flow, and surface tension. Biological molecules suspended in fluid and transported through microfluidics channels interact with the channel-wall material [1,2]. This interaction is even stronger in high surface-area-to-volume ratio (SAVR) microfluidic channels.

Currently large numbers of materials are used in microfluidic chip production including silicon, glass, various plastics and others. Adsorption and inhibition of biomolecules occur when these materials come in contact with biomolecular reaction components. Both adsorption and inhibition are problems that best be avoided because the reaction will not be successful even when one of the components will be inhibited [1,3]. Polymerase chain reaction (PCR) is a thermal cycling procedure for amplifying target DNA. The PCR compatibility of silicon, silicon dioxide (SiO_2) and other surfaces have been studied; however the results are inconclusive [1,2,4,5].

Usually for protein–surface interaction measurements, bulky and expensive equipment is used, such as atomic force microscopy (AFM), scanning or transmission electron microscopy (SEM, TEM), spectrophotometric protein concentration measurement, Fourier transform infrared spectroscopy (FTIR) or X-ray photoelectron spectroscopy (XPS). Further, tests like SEM, TEM and XPS must be performed in vacuum, where water is removed from the sample [6–9]. Although AFM works at ambient temperature, even in liquid the surface is visualized only over a very small area [7,8,10–12]. FTIR is suitable only for micro-samples, allowing the molecular bond and grouping vibrations to be deducted [7,13–16].

We designed a simple, relatively quick measurement that only requires a PCR cycler; thus it mimics actual conditions in PCR cycling. In our study, we evaluated the inhibitory affect of different materials on PCR, which is one of the most frequently used enzymatic reactions in microfluidics [7,17–21]. The PCR reaction components include the DNA template, primers, DNA polymerase (polymerase), dNTPs, a buffer, divalent ions ($MgCl_2$), and KCl. The main component in this reaction is heat-stable polymerase. PCR consists of 20–40 of repeated cycles, with temperature transitions

Abbreviations: RBI, relative band intensity; SAVR, surface-area-to-volume ratio; WRBI, weighted RBI.

* Corresponding author at: Division of Physical Sciences and Engineering, 4700 King Abdullah University of Science and Technology, Thuwal 23955-6900, Saudi Arabia. Tel.: +966 2 8084556; fax: +966 2 8020140.
E-mail addresses: rimantas.kodzius@kaust.edu.sa, kodzius@gmail.com (R. Kodzius), xiaokang@ustc.edu (K. Xiao), ian.foulds@kaust.edu.sa (I.G. Foulds), phwen@ust.hk (W. Wen).

0925-4005/$ – see front matter © 2011 Elsevier B.V. All rights reserved.
doi:10.1016/j.snb.2011.10.044

between ~55 °C and ~95 °C. Current developments allow for temperature cycling between ~71 °C and ~91 °C or even lower temperatures [22]. Lower T_d, enables a wider choice of materials for the PCR.

Initially, most PCR microfluidic devices were fabricated from silicon, as effective technologies had been derived directly from semiconductor fabrication. More recently, owing to demands for specific optical characteristics, bio- or chemical compatibility, lower production costs, and faster prototyping microfluidics, glass, polymers and other materials have been utilized instead.

Adsorption to silica surfaces is caused by the selective action of SiO_x–surface silanol (Si–OH) groups on polar molecules, which is itself a result of a combination of ionic and hydrogen bonding effects. As such, polar molecules such as DNA and the polymerase can be adsorbed by chip material. As early as 1996, Shoffner et al. noted some surface interaction in PCR [1]. Taylor suggested adding carrier-protein bovine serum albumin (BSA) to the PCR mix to compete with Taq polymerase for adsorption at the chip walls [2]. BSA is thought to compete with the polymerase for adsorption at the chip walls and, thus, to improve PCR yields [2]. The adsorption mechanism of Taq polymerase [11] and BSA protein [9,23] has been extensively studied. BSA also acts as a polymerase competitor in the inhibitor chelation [24]. Additionally, BSA facilitates primer annealing, stabilizes both the DNA and the polymerase, and, in so doing, acts as an osmo-protectant. In subsequent years, many more adjuvants, along with passive and active coating strategies, have been investigated [21]. Jeyachandran et al. showed that BSA molecules can be adsorbed to both hydrophobic and hydrophilic surfaces [23] with differing adsorption mechanisms and rates [9]. Prakash et al. systematically studied polymerase adsorption on 13 materials [11], but this study did not use actual PCR conditions, and thus the results are not necessarily translatable to PCR compatibility due to the temperature dependence of adsorption. And while a variety of materials have been tested for PCR compatibility [11], our study is the first to investigate a wide range of materials. Some solutions that avoid the problem of inhibitory effects of certain materials' in enzymatic reactions, such as PCR, have been reported [21,25]. For example, material surface passivation can be achieved by passive coating ("static passivation") or by active coating ("dynamic passivation"). In the former, chemical or biological molecules are applied to the microchannel surface prior to the PCR reaction; in the latter, additives are included in the reaction mix. Passivation techniques are well described in reviews of Zhang et al. [21,25].

To access the material inhibitory properties, we decided to perform only dynamic passivation using BSA, the most common adjuvant in microfluidic PCR. Adsorption of BSA to both charged and hydrophobic surfaces has been assessed widely [23]. Other chip-surface-treatment materials act in a similar way – limiting the access of reaction components to the surface. All of our PCR reaction solutions contained adjuvant betaine, a common additive in most PCR commercial optimization kits [26]. Betaine acts as an osmoprotectant for polymerase, thereby increasing its resistance to denaturation.

PCR reaction optimization through choice of surface materials is of the upmost importance, as it enables and improves enzymatic reaction in microfluidics. Our assessment of the PCR compatibility of various materials commonly used while producing microfluidic devices is also pertinent and beneficial to other enzymatic reactions in microfluidic devices.

2. Materials and methods

2.1. Materials investigated

The following materials were tested for PCR compatibility: polymethyl-methacrylate (PMMA) (cast acrylic sheets Clarex A from Nitto Jushi Kogyo Co. Ltd.), polycarbonate (PC), polyvinyl chloride (PVC), polypropylene (PP, from a 200 μl PCR tube), polytetrafluoroethylene (PTFE), cured polydimethylsiloxane (PDMS), three kinds of wax with melting temperatures (T_m) of 56 °C (white wax: paraffin from Nacalai Tesque), 60 °C (yellow wax: shiftwax from Nikka Seiko) and 80 °C (black wax: wax W from Apiezon), silicon (origin silicon wafer), SiO_2 of 560 nm thickness (carrier silicon wafer), quartz, pyrex glass, indium tin oxide (ITO) glass, soda-lime glass, cured SU-8 epoxy-based negative photoresist (SU-8), Norland Optical Adhesives 61 (NOA61) and 68 (NOA68) exposed to ultraviolet light (UV) light for 2 min, dried epoxy and acrylic glues, metallic iron tubes 0.9 mm in diameter and 12.9 mm in length, and mineral oil for molecular biology (Sigma). Ten microliters of mineral oil were used in the pertinent PCR compatibility test. The other solid materials were manually broken into small fragments using surgical scissors, and a sample of size >5 mm^3 was added to each PCR reaction tube. Assuming (according to our observations) that the sample was fragmented into more than 10 and up to 100 pieces, we calculated the total surface area of the material to be in the range of 4.7×10^1–1.8×10^2 mm^2. For the 10 μl mineral oil used, the total surface area was ~3.5×10^1 mm^2. Due to different material mechanical properties, fragmentation did not result in the same size fragments; therefore it is difficult to provide precise SAVR. The approximate calculated value of SAVR for used materials varies from 9.4×10^0 to 3.5×10^1 $mm^2/\mu l$ (oil SAVR value was ~3.5×10^0 $mm^2/\mu l$). That is an order of magnitude higher than for the SAVR of 1.5×10^0 $mm^2/\mu l$ in a conventional PCR reaction tube (e.g., Perkin-Elmer MicroAmp Reaction Tube) [1].

2.2. PCR methodology

PCR is used to amplify selected sections of DNA. Two-temperature PCR is fast, efficient, and applicable to varying conditions. For current primer pair, the optimized conditions were T_a = 71 °C and T_d = 91 °C. The PCR was performed as published in [22,27], except than the final concentrations for the primers were 0.75 μM and for the SpeedStar HS DNA polymerase they were 0.025 U/μl. Distinguishing the inhibitory effect of strongly inhibiting materials would be difficult if the PCR reaction volume is low. Basically, the reaction would be immediately inhibited without noticing the difference between various materials. To clearly distinguish the inhibitory effect of strong inhibitors the PCR reaction volume was set at 30 μl. This volume also facilitated recovering the PCR mix after incubation with the material.

Detecting the PCR product was achieved by running samples in 4% agarose gel containing SYBR Safe DNA stain (Life Technologies) and by subsequent gel imaging. The band relative intensity was quantified using ImageJ version 1.43 software (developed at the National Institutes of Health) by subtracting the background noise level, etc. and measuring the area of the peak. The obtained value for the band intensity was defined as the relative band intensity (RBI). To relate the RBI to the surface area and the volume of the material, we also defined the weighted RBI (WRBI) as the ratio between RBI and SAVR. The WRBI helps to clarify possible variations in the results, and it reduces the uncertainty introduced by our fracturing method on the SAVR.

2.3. Total reaction inhibition experiment

As indicated in Fig. 1, two PCR master mixes were prepared and distributed among 24 wells in a 96-well plate. The first PCR mix was prepared without BSA; the second contained BSA at a final concentration of 2 μg/μl. The PCR mix was added to the material fragments to test the PCR compatibility. The tubes were briefly vortexed to mix the material with the PCR solution, incubated on ice for 30 min, and then PCR was performed on a bench thermocycler. The

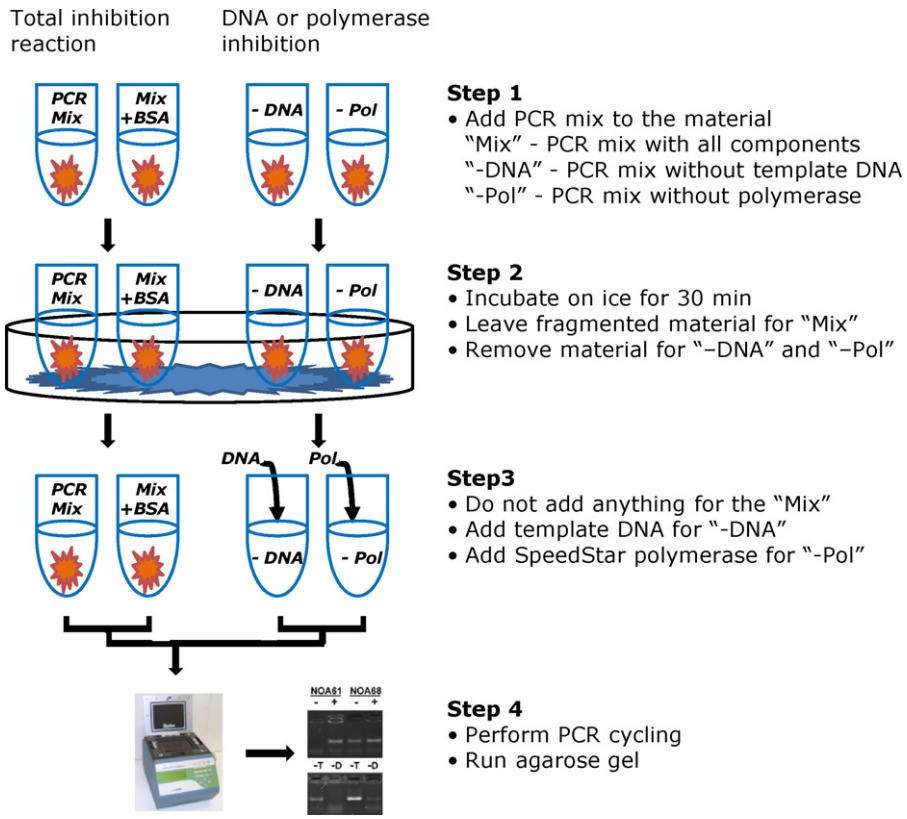

Fig. 1. The PCR compatibility assay. Both the total reaction inhibition experiment and DNA or polymerase adsorption experiments are described. The PCR is performed using bench thermocycler, and subsequent imaging is done on agarose gel. The control experiment was done running PCR without including any of material ("no additives" part, see Fig. 2).

method we used to determine which PCR component was inhibited by our tested materials was to simply omit one of the PCR components during the PCR setup. The component was then added and incubated with the tested material for 30 min. Usual PCR preparation times do not exceed more than 30 min. Additionally, for up to 2 h we do not expect changes in adsorption, because previous research shows that BSA adsorption is restricted to a monolayer with incubation times of less than 2 h [28]. The highest temperature reached in two-temperature PCR was 91 °C. With an even higher T_d, we expect stronger material inhibition on PCR, as multiple sources have shown that amount of surface adsorbed proteins increases at elevated temperatures [29–32]. With two-temperature PCR we could use a lower T_d [33], which would enable a wider choice of materials for the PCR. After PCR, the materials were removed and, for visualization, the amplification products were loaded directly onto the gel.

2.4. DNA and polymerase adsorption experiments

After extracting the PCR mixture, the missing PCR component was added to complete the PCR mixture. PCR was performed to determine if the signal was as intense as the control PCR. If the signal is at the same intensity, then the component under test, which was incubated with the tested material, was not adsorbed. A diminished signal indicates that the material adsorbs some of PCR component under test, as that particular PCR component was incubated with the tested materials.

As shown in Fig. 1, two different PCR mixes were prepared, both without additive BSA. For the DNA adsorption experiment, the PCR mix was prepared without the polymerase, whereas, for the polymerase adsorption experiment, template DNA was omitted. Thirty microliters of the PCR mix was distributed into tubes containing fragmented material. The tubes were briefly vortexed in order to mix the PCR solution with the material, after which they were incubated on ice for 30 min. Then, 10 μl of the PCR mix, separated from the material, was extracted and transferred to the new tubes. A 0.3 μl (1.5 U) quantity of the SpeedStar polymerase was added to the tubes lacking the polymerase. One microliter (corresponding to 2,000,000 dsDNA molecules) of template solution was added to the tubes with the PCR mixture lacking template DNA. PCR was performed with the cycling conditions T_a = 71 °C and T_d = 91 °C each for 20 s, for 35 cycles. The products were then loaded onto the gel for visualization.

3. Results and discussion

3.1. PCR inhibition phenomena

Although some literature reports ideal BSA concentrations ranging between 0.5 and 1.0 μg/μl, BSA has been utilized on chips at concentrations as high as 2.5 μg/μl [2,24,34,35]. In fact, in our present experiments, the positive controls revealed that BSA at the 2 μg/μl concentration had no negative influence on the PCR. Previous research showed that BSA adsorption is restricted to a monolayer with incubation times of less than 2 h and at concentrations lower than 10 μg/μl [28].

To assess a material's compatibility with PCR, we included a wide range of materials used in microfluidics. PCR with those materials, but without BSA, revealed which materials are PCR-inhibitory. Successful PCR produces more DNA; the fluorescent band on the gel is more intense, and, therefore, the RBI value is higher. When measuring and quantifying the values of RBI, virtually no signal (RBI < 1.9×10^2) was detected in PCR with PMMA, waxes (T_m 56 °C and 60 °C), ITO glass, SU-8, NOA61, epoxy, and acrylic glues. Only

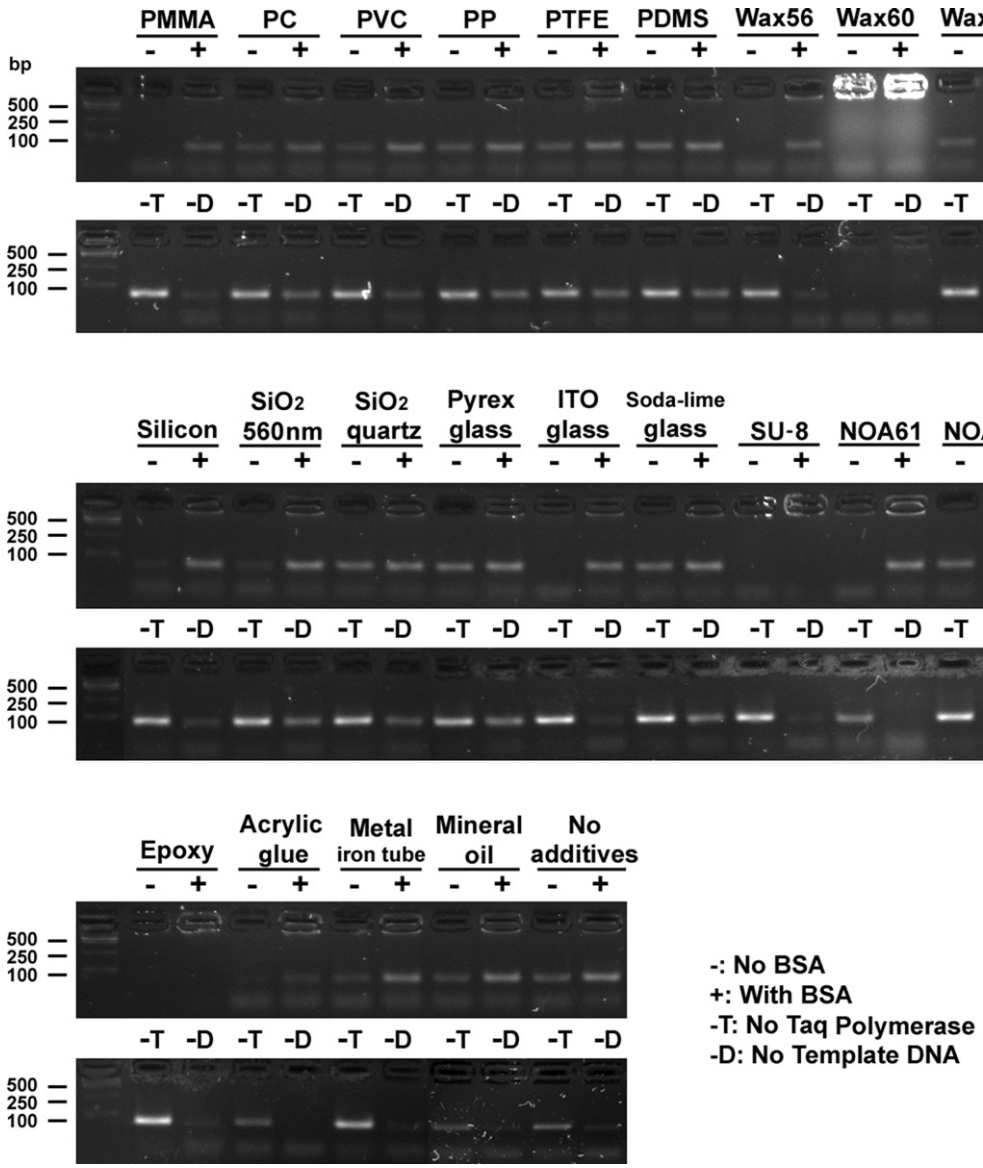

Fig. 2. Amplification of 71 bp CMV fragment. More intense band indicates successful PCR (no or little material inhibition).

a weak signal (RBI < 8.4×10^2) was obtained in PCR with PC, PVC, silicon, silicon with a layer of 560 nm SiO_2, and the metal tubes. However, if BSA was included in the PCR mix, a strong signal (RBI > 1.4×10^3) was obtained for the PMMA, PC, PVC, wax (T_m 56 °C), silicon, silicon with a layer of 560 nm SiO_2, SiO_2 quartz, ITO glass, NOA61, and the metal tubes. We conclude, therefore, that wax (T_m 60 °C) (RBI = 1.9×10^2), SU-8 (RBI = 5.5×10^1), and the epoxy glue (RBI = 1.1×10^2) are PCR-inhibitory with or without additive BSA. Most PCR-friendly materials exhibit similar signals regardless of the inclusion or not of BSA in the PCR mixture; these materials are PP, PTFE, PDMS, wax (T_m 80 °C), SiO_2 quartz, pyrex and soda-lime glasses, NOA68, and mineral oil (Figs. 2 and 3 and Table 1).

Next, we determined which reaction components are inhibited by the included materials. Theoretically, every PCR reaction component could be tested for possible inhibition within microfluidics channels; however, we decided to restrict the choice to the testing of materials possibly inhibitory of the key components of the PCR mixture, which are the DNA and the polymerase. In order to simulate natural PCR conditions, BSA was not included in the PCR mixture.

The PCR reaction contains template DNA, primers and free dNTPs. Since primers and dNTP are in excess, we concentrated on template DNA. Also, template DNA is much longer than either primers or dNTP. Thus, if template DNA were adsorbed, the shorter DNA molecules would be adsorbed as well, due to the kinetic nature of adsorption (i.e., smaller molecules are more prone to being adsorbed).

Our results showed that there was near total adsorption of template DNA when the wax (T_m 60 °C) was used (RBI = 9.2×10^1). In contrast, when NOA61, mineral oil and acrylic glue materials were employed, significant adsorption occurred (RBI < 1.5×10^3). As shown in Figs. 2 and 4 and Table 2, the other examined materials did not exert any noticeable effect on the template DNA (RBI > 3.0×10^3). DNA is a polyanionic molecule; therefore, it is not expected to bind to hydrophobic surfaces [36]. Our observation that DNA is not adsorbed in noticeable amounts is in agreement with the previous literature [37]. Additional inhibitors that reduce the final PCR product by interacting with DNA, such as humic acid, collagen, and melanin, are also discussed in [37]. Some inhibitors, such as hematin and melanin, might affect the processivity (the rate of extension) of the polymerase during primer extension [38].

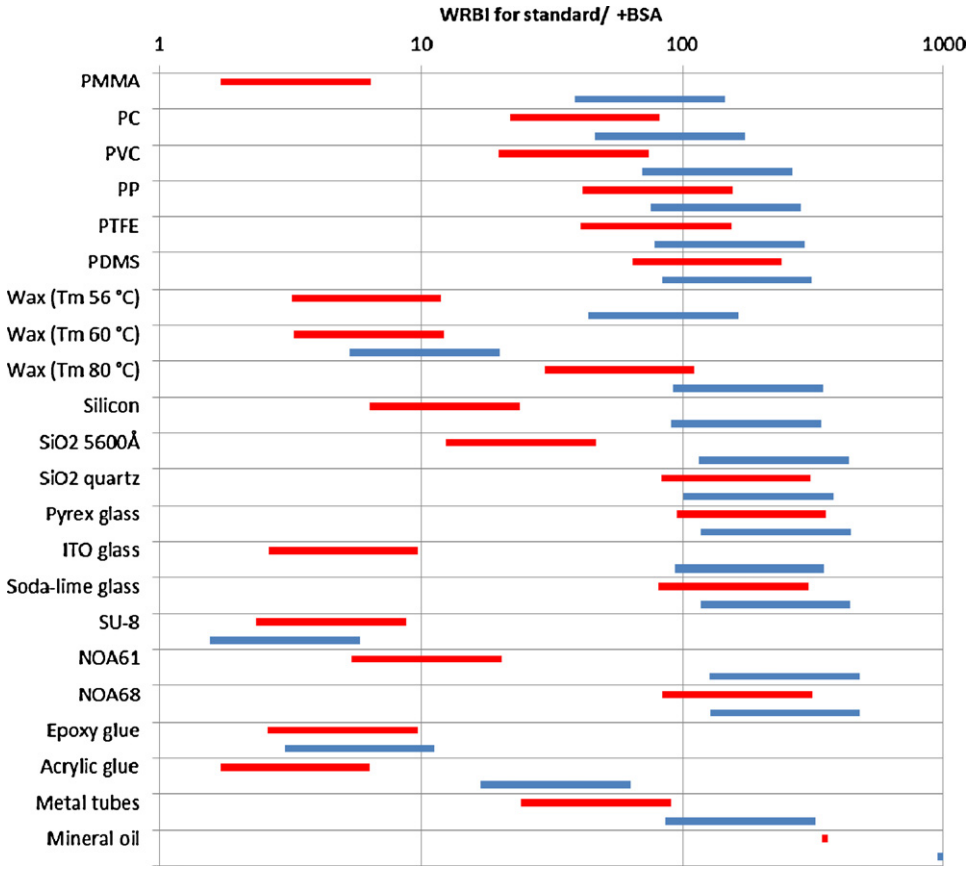

Fig. 3. PCR inhibition through various materials. Comparison of PCR mix without BSA (red bars) or containing BSA (blue bars). The calculated WRBI range is indicated for each of material. Lower WRBI values indicate inhibition, whereas higher WRBI values means less inhibition. (For interpretation of the references to color in this figure legend, the reader is referred to the web version of the article.)

We characterized the SpeedStar polymerase adsorption onto the investigated materials. Here, we observed more significant effects on the PCR efficiency. The polymerase-inhibition experiments indicate that following materials do not have strong effects (RBI > 1.1×10^3) on polymerase: PC, PP, PTFE, PDMS, silicon with a layer of 560 nm SiO_2, SiO_2 quartz, pyrex, and soda-lime glass. Slight polymerase inhibition (RBI < 9.2×10^2) was observed with PMMA, PVC, waxes (T_m 56 °C and 80 °C), silicon, and NOA68. A very strong or near total inhibition (RBI < 1.8×10^2) was observed with wax (T_m 60 °C), ITO glass, SU-8, NOA61,

Table 1
PCR inhibition through various materials. Comparison of PCR mix without BSA or containing BSA. The measured RBI and calculated range of WRBI are indicated. N.A.—not applicable.

Material	RBI, standard	WRBI, standard	RBI, +BSA	WRBI, +BSA
PMMA	6.0×10^1	1.7×10^0~6.4×10^0	1.4×10^3	3.9×10^1~1.5×10^2
PC	7.7×10^2	2.2×10^1~8.2×10^1	1.6×10^3	4.6×10^1~1.7×10^2
PVC	6.9×10^2	2.0×10^1~7.4×10^1	2.5×10^3	7.1×10^1~2.6×10^2
PP	1.4×10^3	4.1×10^1~1.5×10^2	2.7×10^3	7.6×10^1~2.8×10^2
PTFE	1.4×10^3	4.1×10^1~1.5×10^2	2.8×10^3	7.9×10^1~2.9×10^2
PDMS	2.2×10^3	6.4×10^1~2.4×10^2	2.9×10^3	8.4×10^1~3.1×10^2
Wax (T_m 56 °C)	1.1×10^2	3.2×10^0~1.2×10^1	1.5×10^3	4.4×10^1~1.6×10^2
Wax (T_m 60 °C)	1.1×10^2	3.3×10^0~1.2×10^1	1.9×10^2	5.3×10^0~2.0×10^1
Wax (T_m 80 °C)	1.0×10^3	3.0×10^1~1.1×10^2	3.2×10^3	9.2×10^1~3.5×10^2
Silicon	2.2×10^2	6.4×10^0~2.4×10^1	3.2×10^3	9.1×10^1~3.4×10^2
SiO_2 5600 Å	4.4×10^2	1.3×10^1~4.7×10^1	4.1×10^3	1.2×10^2~4.3×10^2
SiO_2 quartz	2.9×10^3	8.3×10^1~3.1×10^2	3.5×10^3	1.0×10^2~3.8×10^2
Pyrex glass	3.3×10^3	9.5×10^1~3.6×10^2	4.1×10^3	1.2×10^2~4.4×10^2
ITO glass	9.1×10^1	2.6×10^0~9.7×10^0	3.3×10^3	9.4×10^1~3.5×10^2
Soda-lime glass	2.8×10^3	8.1×10^1~3.0×10^2	4.1×10^3	1.2×10^2~4.4×10^2
SU8	8.2×10^1	2.4×10^0~8.8×10^0	5.5×10^1	1.6×10^0~5.9×10^0
NOA61	1.9×10^2	5.4×10^0~2.0×10^1	4.5×10^3	1.3×10^2~4.8×10^2
NOA68	2.9×10^3	8.4×10^1~3.2×10^2	4.5×10^3	1.3×10^2~4.8×10^2
Epoxy glue	9.1×10^1	2.6×10^0~9.7×10^0	1.1×10^2	3.0×10^0~1.1×10^1
Acrylic glue	6.0×10^1	1.7×10^0~6.4×10^0	5.9×10^2	1.7×10^1~6.4×10^1
Metal tubes	8.4×10^2	2.4×10^1~9.0×10^1	3.0×10^3	8.6×10^1~3.2×10^2
Mineral oil	1.2×10^3	3.4×10^2~3.6×10^2	3.4×10^3	9.4×10^2~1.0×10^3
No additives	1.8×10^3	N.A.	4.1×10^3	N.A.

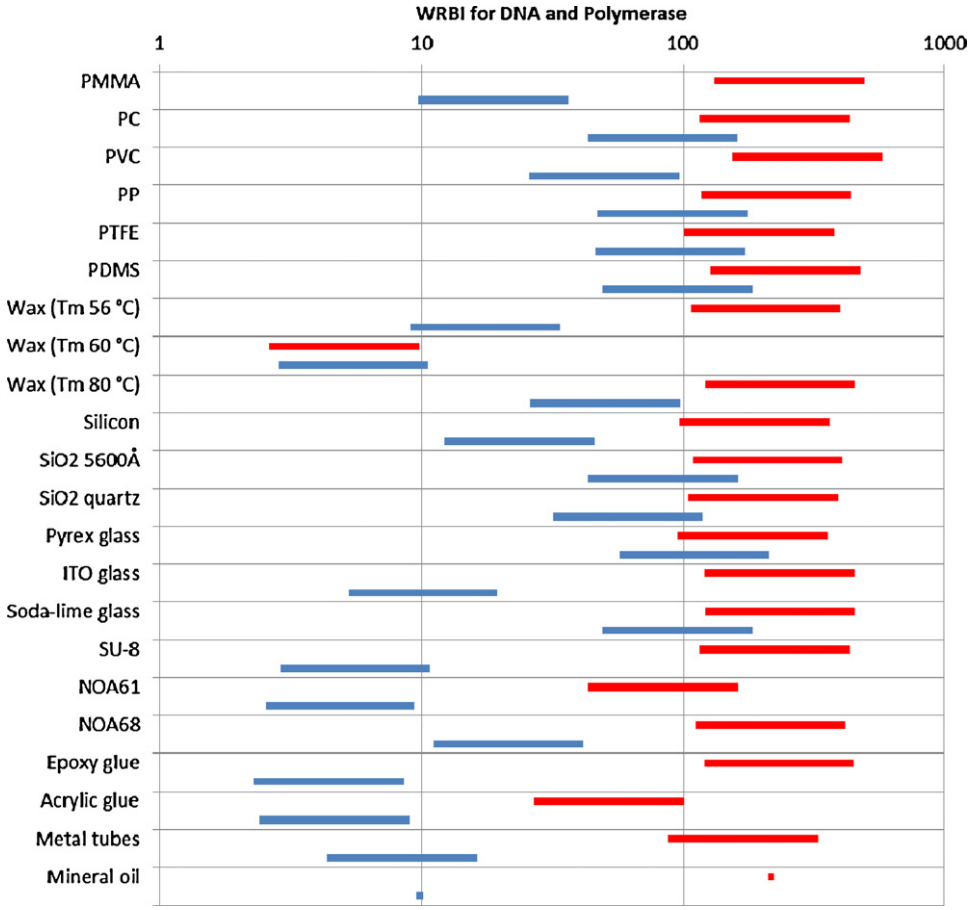

Fig. 4. PCR inhibition through material interaction with template DNA—where the polymerase has been added after the rest of the PCR mix has been incubated with the material under test. This is to avoid interaction between the material under test and the polymerase (red bars). PCR inhibition through material interaction with polymerase—where the DNA has been added after the rest of the PCR mix has been incubated with the material under test. This is to avoid interaction between the material under test and the DNA (blue bars). The calculated WRBI range is indicated for each of material. Lower WRBI values indicate inhibition, whereas higher WRBI values means less inhibition. See Section 2.4 for further description of the method. (For interpretation of the references to color in this figure legend, the reader is referred to the web version of the article.)

metal tubes, mineral oil, epoxy, and the acrylic glues (Fig. 2 and Table 2).

The possible variation of the SAVR between different materials due to the fracturing process leads to a limited estimate of the SAVR. Without a precise estimate of the SAVR, the components listed in Tables 1 and 2 should be compared with caution. The difference for PCR-compatibility may be also due to the SAVR; i.e., a slightly incompatible material with a high SAVR might appear worse than a very incompatible material with a low SAVR. To this end, the WRBI values have been plotted to provide an estimate of the uncertainty present in the measurements (Figs. 3 and 4).

3.2. Material inhibitory effect

Silicon has been widely used to fabricate PCR chips, as it has a very high thermal conductivity and is easy to fabricate. Our finding that bare silicon has a stronger inhibitory effect on the polymerase than SiO_2 (RBI = 2.2×10^2 versus RBI = 4.4×10^2 without BSA) is in line with the literature [1,2,4]. Surprisingly, SiO_2 quartz (RBI = 2.9×10^3), which already has been used in microfluidics [39–41], does not have as strong of an effect as silicon or silicon with a 560 nm layer of SiO_2. Because SiO_2 has at least 12 crystalline forms [42] which may be produced by both oxidation or chemical reaction deposition, its inhibition properties need further investigation.

We also compared three kinds of oxides: pyrex, soda-lime, and ITO. According to earlier findings, pyrex and soda-lime glasses (RBI = 3.3×10^3 and 2.8×10^3, respectively) allow amplification without additive BSA [7], whereas ITO glass requires that BSA be included in the PCR mix (RBI = 9.1×10^1 without BSA and 3.3×10^3 with BSA) [43]. SU-8 was found to be inhibitory both with and without BSA (RBI < 8.2×10^1) in the PCR mixture. Untreated SU-8 had already been shown to be inhibitory [11,44].

NOA61 and NOA68 are liquid photopolymers that are cured by exposure to UV. Whereas NOA61 is more suitable as an adhesive for glass and metal, NOA68 is an excellent choice for plastics. NOA68 has a higher viscosity (22,000 CPS) than NOA61 (300 CPS). Despite such small differences, commercial product NOA68 is significantly more PCR-friendly than NOA61 (RBI = 2.9×10^3 vs. 1.9×10^2). For the NOA61 material, the PCR amplification was successful only with the additive BSA. Acrylic glue, for its part, is more PCR-friendly than epoxy glue and performs better when BSA is included (RBI = 5.9×10^2), whereas the PCR with the epoxy material was a failure (RBI = 1.1×10^2). Therefore, we recommend that acrylic glue be used instead of epoxy.

Metal tubing reduces the PCR yield through inhibition of the polymerase rather than by binding to template DNA (RBI = 1.5×10^2 vs. 3.0×10^3). Panaro et al. observed that PCR is inhibited with other metals, such as stainless steel, titanium [45], 1.0×10^1 mm^2 surface area platinum [46], and 1.2×10^1 mm^2 gold nanoparticles [47].

Table 2
PCR inhibition through material interaction with template DNA or the polymerase correspondingly. The measured RBI and calculated range of WRBI are indicated. N.A.—not applicable.

Material	RBI, interaction with DNA	WRBI, interaction with DNA	RBI, interaction with polymerase	WRBI, interaction with polymerase
PMMA	4.6×10^3	1.3×10^2~5.0×10^2	3.4×10^2	9.7×10^0~3.6×10^1
PC	4.0×10^3	1.2×10^2~4.3×10^2	1.5×10^3	4.3×10^1~1.6×10^2
PVC	5.4×10^3	1.5×10^2~5.8×10^2	9.1×10^2	2.6×10^1~9.7×10^1
PP	4.1×10^3	1.2×10^2~4.4×10^2	1.7×10^3	4.8×10^1~1.8×10^2
PTFE	3.5×10^3	1.0×10^2~3.8×10^2	1.6×10^3	4.6×10^1~1.7×10^2
PDMS	4.5×10^3	1.3×10^2~4.8×10^2	1.7×10^3	4.9×10^1~1.8×10^2
Wax (T_m 56 °C)	3.7×10^3	1.1×10^2~4.0×10^2	3.2×10^2	9.1×10^0~3.4×10^1
Wax (T_m 60 °C)	9.2×10^2	2.6×10^0~9.8×10^0	1.0×10^2	2.9×10^0~1.1×10^1
Wax (T_m 80 °C)	4.3×10^3	1.2×10^2~4.5×10^2	9.2×10^2	2.6×10^1~9.8×10^1
Silicon	3.4×10^3	9.7×10^1~3.6×10^2	4.3×10^2	1.2×10^1~4.6×10^1
SiO_2 5600 Å	3.8×10^3	1.1×10^2~4.1×10^2	1.5×10^3	4.3×10^1~1.6×10^2
SiO_2 quartz	3.7×10^3	1.0×10^2~3.9×10^2	1.1×10^3	3.2×10^1~1.2×10^2
Pyrex glass	3.3×10^3	9.6×10^1~3.6×10^2	2.0×10^3	5.7×10^1~2.1×10^2
ITO glass	4.2×10^3	1.2×10^2~4.5×10^2	1.8×10^2	5.3×10^0~2.0×10^1
Soda-lime glass	4.3×10^3	1.2×10^2~4.5×10^2	1.7×10^3	4.9×10^1~1.8×10^2
SU8	4.1×10^3	1.2×10^2~4.3×10^2	1.0×10^2	2.9×10^0~1.1×10^1
NOA61	1.5×10^3	4.3×10^1~1.6×10^2	8.1×10^1	2.5×10^0~9.5×10^0
NOA68	3.9×10^3	1.1×10^2~4.2×10^2	3.9×10^3	1.1×10^1~4.2×10^1
Epoxy glue	4.2×10^3	1.2×10^2~4.5×10^2	8.0×10^1	2.3×10^0~8.6×10^0
Acrylic glue	9.4×10^2	2.7×10^1~1.0×10^2	8.4×10^1	2.4×10^0~9.0×10^0
Metal tubes	3.0×10^3	8.7×10^1~3.3×10^2	1.5×10^2	4.4×10^0~1.6×10^1
Mineral oil	7.6×10^2	2.1×10^2~2.2×10^2	3.4×10^1	9.6×10^0~1.0×10^1
No additives	9.8×10^2	N.A.	2.0×10^2	N.A.

To overcome this inhibition, they suggest adding excessive EDTA followed by the same amount of Mg^{2+} [48].

Mineral oil has little influence on PCR performance (RBI = 1.2×10^3 without BSA and 3.4×10^3 with BSA), which is understandable because mineral oil is inert and, as such, does not interact with magnesium ions. Mineral oil has had a long association with PCR; the first thermocyclers used it in place of top heaters to cover PCR mixtures and avoid evaporation. Some polymers treated by native or molecular biology mineral oil may have negative (Buna-N, silicone) or positive (Santoprene) effect on PCR [45]. Because mineral oil has many kinds, we advise that further testing be conducted to determine the best kind for PCR.

Among the six different plastics tested, the least inhibitory are PP, PTFE, and PDMS (RBI > 1.4×10^3 without BSA). Conventional tubes, multiwell plates, and microchips for PCR are fabricated from PP [49]. PTFE is a synthetic fluoropolymer, an inert material that has already been used in microfluidics PCR [18]. PDMS, too, is well known, and it has extensive use in microfluidics, including PCR [46,50,51]. When BSA was included in the reaction mix, PMMA, PC, and PVC were found to be suitable for microfluidics (RBI > 1.4×10^3).

The various waxes do not form a chemically homogeneous group. All waxes are water-resistant materials composed of various substances, including long-chain (from 12 to 38 carbon atoms), hydrocarbons, ketones, alcohols, aldehydes, sterol esters, alkanoic acids, terpenes, and monoesters, which are solid over a wide temperature range. Wax, not only chemically, but also some of its by-products, can influence PCR performance. Because wax has been receiving more attention in the microfluidics field, we included it in our assay [22,52–55]. We tested three kinds of wax obtained from three companies. We observed that wax with T_m = 80 °C is the most PCR-compatible (RBI = 1.0×10^3 without BSA and 3.2×10^3 with BSA). Also, amplification could be performed by adding BSA (RBI = 1.5×10^3) when using wax with T_m = 56 °C. Wax with T_m = 60 °C, however, was found not to be compatible with the PCR reaction, as it totally inhibited the reaction despite the inclusion of BSA (RBI = 1.9×10^2). In our previous work, we demonstrated that wax with T_m = 60 °C still can be used for PCR by doubling the polymerase concentration [22].

This study of the inhibitory effect of various common microfluidics materials has provided a new rapid testing method using only a PCR cycler, and it has confirmed and expanded the list of tested materials.

3.3. Achieving successful PCR

In this publication, we provide a simple method for analyzing the inhibition mechanism (DNA template loss versus polymerase loss) that enables the extrapolation of a material's PCR compatibility from this work to other studies.

Indeed, the simple PCR inhibition test described herein can be used to choose the most friendly microfluidics materials or to evaluate the wide range of additives to be included in PCR. In our experiments, we demonstrated that BSA enhances the PCR product yield for most of the tested materials; the most visible effects (RBI change difference is more than 9 times) were with PMMA, wax (T_m = 56 °C), silicon, silicon with a layer of 560 nm SiO_2, ITO glass, NOA61, and acrylic glue. Some polymerases were adsorbed on the surface more than others [7], but, by increasing the DNA or the polymerase concentration, PCR amplification products were obtained even without any additives (results not shown). In such cases, the entire DNA or the polymerase was probably not inhibited or adsorbed, so the remaining free DNA or polymerase was sufficient for successful amplification. Regardless, careful selection of the right PCR components helps to improve the product yield. Further, oil, in the form of water-in-oil droplets, helps to minimize the contact of PCR reaction components with wall materials, and, because mineral oil is non-inhibitory, we advise using it. Additionally, due to the effectively reduced interaction between materials and the PCR components, two-temperature PCR with a low denaturing temperature (T_d) allowed for wider material choice in chip production. Employing real-time PCR, moreover, could help understand the general mechanism of that interaction. Real-time PCR experiments have been conducted for Si and SiO_2 inhibitory effects [5], as well as to determine the effects on the various PCR inhibitors [38].

Quantifying the PCR compatibility of the tested materials is possible by measuring the SAVR and relating it to the changes of the PCR outcome. Although obtaining powder of various materials by physically smashing is possible, this method makes estimating

the SARV difficult. The surface area of nanoparticles as small as 5 nm can be easily calculated and the area can be correlated to the PCR inhibitory effect. Wan et al. showed that the PCR product yield is modulated by the total surface area of gold nanoparticles regardless of the size [47]. Gonzales et al. tested tubing of various fluoropolymers. He concluded that tubing up to 40 cm (internal diameter 5.0×10^2 μm, inner surface area 6.3×10^2 mm^2) can be used safely, while the longer tubing of 3 meters (inner surface area 4.7×10^3 mm^2) adsorbs the DNA and Sybr Green I, a DNA stain substantially to the tubing walls resulting to severely subsequent PCR inhibition [56]. Knowing the tubing diameter, the surface area can be calculated. For example, the surface area of conventional 200 μl PCR tube is 3.0×10^1 mm^2. However, its not easy to obtain tubing of some materials and perform test PCR for inhibition. Panaro et al. machined a 1 mm diameter and 25 mm long channel into plastic materials, for the incubation of PCR mixture. He also used a 16-gauge punch to cut small pieces of gasket material in diameter of 1 mm with a total surface area of 4.0×10^1 mm^2 [45]. Our inhibition investigation method provided means for a fast PCR inhibition test of a wider range of materials than previously tested. The results are suitable for semiquantitative measuring of inhibition, as choosing similar amounts of various materials will provide only an estimate value of SAVR (the total material surface area was 4.7×10^1–1.8×10^2 mm^2). However, our method is well suitable for indicating materials that are severely problematic for microfluidics. In a higher SAVR environment, more DNA or polymerase may be needed to avoid the inhibitory effect, as even seemingly friendly materials may become problematic due to the adsorption of PCR components. In our current study, only PCR with the addition of 60 °C yellow wax did not yield any amplification. We already demonstrated the total reaction inhibition phenomenon for various paper materials impregnated with wax or acrylic glue. Although we chose a lower end polymerase concentration of 0.025 U/μl, the polymerase concentration can be doubled to 0.05 U/μl [22,27]. At present, a wide variety of plastics is used for microfluidics, and we expect additional materials, such as paper-based chips, to be introduced in the near future [22,27,53,54,57–61].

Our results show that material selection for microfluidic PCR chips, which are characterized by large SAVR, is a vital part of optimizing PCR outcome. For example, an SU-8 based microfluidic PCR system would be expected to provide less than one tenth of the signal (WRBI 1.6×10^0–5.9×10^0) as the same system fabricated in PDMS (WRBI 4.4×10^1–1.6×10^2). Thus material selection is as important an optimization parameter, as primer and polymerase selection or reaction component and conditions (temperature, time) optimization [33]. The type of PCR compatibility test treated in this paper enables the most effectual choice of materials for use in biology-related experiments.

4. Conclusions

As part of the current miniaturization trend, biological reactions and processes are being adapted to microfluidics devices. Because PCR is the primary method employed in DNA amplification, its miniaturization is central to efforts to develop portable devices for diagnostics and testing purposes. A problem, however, is the PCR-inhibitory effect due to the interaction between PCR reagents and the surrounding environment, the effects of which are increased in high-SAVR microfluidics. Some materials are poorly standardized with batch-to-batch variations. In this study, we introduced a simple test for assessing the compatibility of materials in PCR. Because of its speed and simplicity, we have been able to compare the PCR compatibility of a wider range of materials than any previous study. This test does not require bulky or expensive equipment used for protein–surface interaction measurements, such as AFM, SEM or TEM, spectrophotometric protein concentration measurement, FTIR or XPS. Our test can be easily conducted in common PCR tubes using a standard bench thermocycler available in every molecular biology laboratory in order to clearly identify materials that inhibit the PCR reaction components. The PCR component adsorption is assessed in natural PCR conditions, during the cycling in high temperatures. The test can be performed on a large number of material samples in parallel, and a database of tested materials can be created and shared. Furthermore, the biocompatibility of materials can be measured on a DNA, RNA, enzymatic (protein) or cellular level.

In keeping with other work in the literature, we confirmed that including BSA in the PCR reaction can significantly improve most of the tested materials' surface compatibility, which improves reaction performance and yield outcomes. This finding is especially important because most biological reactions occur on the surface. Our proposed strategy for material-surface PCR compatibility testing can be used for other biological processes as well. Such compatibility is central to every such process. A similar test can be performed for cell studies measuring the inhibition of materials on cell growth [10,63]. In such a test, both the cells and the cell medium components can be tested for the adsorption on the material surface. Thus other applications, for example, high-throughput screening [64,65] or transcriptome analysis [66,67] could benefit from our described approach.

Acknowledgements

The authors would like to acknowledge the financial support provided by the Hong Kong Research Grants Council (Grant No. HKUST 603208 and 660207). This paper is based on work partially supported by Award No. SA-C0040/UK-C0016 made by King Abdullah University of Science and Technology (KAUST).

References

[1] M.A. Shoffner, J. Cheng, G.E. Hvichia, L.J. Kricka, P. Wilding, Chip PCR. I. Surface passivation of microfabricated silicon-glass chips for PCR, Nucleic Acids Res. 24 (1996) 375–379.
[2] T.B. Taylor, E.S. Winn-Deen, E. Picozza, T.M. Woudenberg, M. Albin, Optimization of the performance of the polymerase chain reaction in silicon-based microstructures, Nucleic Acids Res. 25 (1997) 3164–3168.
[3] P. Wilding, M.A. Shoffner, L.J. Kricka, PCR in a silicon microstructure, Clin. Chem. 40 (1994) 1815–1818.
[4] J. Cheng, M.A. Shoffner, G.E. Hvichia, L.J. Kricka, P. Wilding, Chip PCR. II. Investigation of different PCR amplification systems in microfabricated silicon-glass chips, Nucleic Acids Res. 24 (1996) 380–385.
[5] W. Wang, H. Wang, Z. Li, Z. Guo, Silicon inhibition effects on the polymerase chain reaction: a real-time detection approach, J. Biomed. Mater. Res. A 77 (2006) 28–34.
[6] M. Bovi, N. Gassler, B. Hermanns-Sachweh, Determination of the biocompatibility of biomaterials by scanning electron microscopy (SEM), in: S. Richter, A. Schwedt (Eds.), EMC 2008 14th European Microscopy Congress 1–5 September 2008, Springer Berlin Heidelberg, Aachen, Germany, 2008, pp. 727–728.
[7] C. Potrich, L. Lunelli, S. Forti, D. Vozzi, L. Pasquardini, L. Vanzetti, C. Panciatichi, M. Anderle, C. Pederzolli, Effect of materials for micro-electro-mechanical systems on PCR yield, Eur. Biophys. J. 39 (2010) 979–986.
[8] R. Subbiah, H. Lee, M. Veerapandian, S. Sadhasivam, S.-W. Seo, K. Yun, Structural and biological evaluation of a multifunctional SWCNT-AgNPs-DNA/PVA bionanofilm, Anal. Bioanal. Chem. 400 (2011) 547–560.
[9] B. Sweryda-Krawiec, H. Devaraj, G. Jacob, J.J. Hickman, A new interpretation of serum albumin surface passivation, Langmuir 20 (2004) 2054–2056.
[10] D. Deryabin, A. Vasilchenko, E. Aleshina, A. Tlyagulova, H. Nikiyan, An investigation into the interaction between carbon-based nanomaterials and and *Escherichia coli* cells using atomic force microscopy, Nanotechnol. Russ. 5 (2010) 857–863.
[11] A.R. Prakash, M. Amrein, K.V.I.S. Kaler, Characteristics and impact of Taq enzyme adsorption on surfaces in microfluidic devices, Microfluid. Nanofluid. 4 (2007) 295–305.
[12] A. Zarubina, E. Lukashev, L. Deev, I. Parkhomenko, A. Rubin, Biotesting the biological effects of single-wall carbon nanotubes using bioluminescent bacteria test-system, Nanotechnol. Russia 4 (2009) 871–875.

[13] A.K. Dutta, A. Nayak, G. Belfort, Viscoelastic properties of adsorbed and cross-linked polypeptide and protein layers at a solid–liquid interface, J. Colloid Interface Sci. 324 (2008) 55–60.
[14] C.E. Giacomelli, M.G. Bremer, W. Norde, ATR-FTIR study of IgG adsorbed on different silica surfaces, J. Colloid Interface Sci. 220 (1999) 13–23.
[15] A. Khandwekar, D. Patil, Y. Shouche, M. Doble, The biocompatibility of sulfobetaine engineered polymethylmethacrylate by surface entrapment technique, J. Mater. Sci.: Mater. Med. 21 (2010) 635–646.
[16] C. Tao, J. Zhang, S. Yang, Preparation and biocompatibility of BSA monolayer on silicon surface, J. Nanosci. Nanotechnol. 11 (2011) 5068–5074.
[17] M.C. Carles, N.J. Sucher, Polymerase chain reaction on microchips, Methods Mol. Biol. 321 (2006) 131–140.
[18] Y. Li, D. Xing, C. Zhang, Rapid detection of genetically modified organisms on a continuous-flow polymerase chain reaction microfluidics, Anal. Biochem. 385 (2009) 42–49.
[19] J. Pipper, M. Inoue, L.F. Ng, P. Neuzil, Y. Zhang, L. Novak, Catching bird flu in a droplet, Nat. Med. 13 (2007) 1259–1263.
[20] N. Szita, K. Polizzi, N. Jaccard, F. Baganz, Microfluidic approaches for systems and synthetic biology, Curr. Opin. Biotechnol. 21 (2010) 517–523.
[21] C. Zhang, J. Xu, W. Ma, W. Zheng, PCR microfluidic devices for DNA amplification, Biotechnol. Adv. 24 (2006) 243–284.
[22] X. Gong, X. Yi, K. Xiao, S. Li, R. Kodzius, J. Qin, W. Wen, Wax-bonding 3D microfluidic chips, Lab Chip 10 (2010) 2622–2627.
[23] Y.L. Jeyachandran, E. Mielczarski, B. Rai, J.A. Mielczarski, Quantitative and qualitative evaluation of adsorption/desorption of bovine serum albumin on hydrophilic and hydrophobic surfaces, Langmuir 25 (2009) 11614–11620.
[24] C.A. Kreader, Relief of amplification inhibition in PCR with bovine serum albumin or T4 gene 32 protein, Appl. Environ. Microbiol. 62 (1996) 1102–1106.
[25] C. Zhang, D. Xing, Miniaturized PCR chips for nucleic acid amplification and analysis: latest advances and future trends, Nucleic Acids Res. 35 (2007) 4223–4237.
[26] S. Frackman, G. Kobs, D. Simpson, D. Storts, Betaine and DMSO enhancing agents for PCR, Promega Notes 65 (1998) 27.
[27] X. Yi, R. Kodzius, X. Gong, K. Xiao, W. Wen, A simple method of fabricating mask-free microfluidic devices for biological analysis, Biomicrofluidics 4 (2010).
[28] R. Ishiguro, Y. Yokoyama, H. Maeda, A. Shimamura, K. Kameyama, K. Hiramatsu, Modes of conformational changes of proteins adsorbed on a planar hydrophobic polymer surface reflecting their adsorption behaviors, J. Colloid Interface Sci. 290 (2005) 91–101.
[29] A. Kondo, H. Fukuda, Effects of adsorption conditions on kinetics of protein adsorption and conformational changes at ultrafine silica particles, J. Colloid Interface Sci. 198 (1998) 34–41.
[30] C.A. Haynes, W. Norde, Globular proteins at solid/liquid interfaces, Colloids Surf. B: Biointerfaces 2 (1994) 517–566.
[31] M. Malmsten, Formation of adsorbed protein layers, J. Colloid Interface Sci. 207 (1998) 186–199.
[32] M. Rabe, D. Verdes, S. Seeger, Understanding protein adsorption phenomena at solid surfaces, Adv. Colloid Interface Sci. 162 (2011) 87–106.
[33] J. Wu, R. Kodzius, K. Xiao, J. Qin, W. Wen, Fast detection of genetic information by an optimized PCR in an interchangeable chip, Biomed. Microdev., doi:10.1007/s10544-011-9595-6, in press, 1–8, Online First 6 October 2011.
[34] B.A. Forbes, K.E. Hicks, Substances interfering with direct detection of *Mycobacterium tuberculosis* in clinical specimens by PCR: effects of bovine serum albumin, J. Clin. Microbiol. 34 (1996) 2125–2128.
[35] T.A. Giambernardi, U. Rodeck, R.J. Klebe, Bovine serum albumin reverses inhibition of RT-PCR by melanin, Biotechniques 25 (1998) 564–566.
[36] J.F. Allemand, D. Bensimon, L. Jullien, A. Bensimon, V. Croquette, pH-dependent specific binding and combing of DNA, Biophys. J. 73 (1997) 2064–2070.
[37] I. Erill, S. Campoy, N. Erill, J. Barbé, J. Aguiló, Biochemical analysis and optimization of inhibition and adsorption phenomena in glass-silicon PCR-chips, Sens. Actuators B: Chem. 96 (2003) 685–692.
[38] K.L. Opel, D. Chung, B.R. McCord, A study of PCR inhibition mechanisms using real time PCR, J. Forensic Sci. 55 (2010) 25–33.
[39] D. Greif, L. Galla, A. Ros, D. Anselmetti, Single cell analysis in full body quartz glass chips with native UV laser-induced fluorescence detection, J. Chromatogr. A 1206 (2008) 83–88.
[40] H. Wang, H.-M. Wang, Q.-H. Jin, H. Cong, G.-S. Zhuang, J.-L. Zhao, C.-L. Sun, H.-W. Song, W. Wang, Microchip-based small, dense low-density lipoproteins assay for coronary heart disease risk assessment, Electrophoresis 29 (2008) 1932–1941.
[41] G. Zhuang, Q. Jin, J. Liu, H. Cong, K. Liu, J. Zhao, M. Yang, H. Wang, A low temperature bonding of quartz microfluidic chip for serum lipoproteins analysis, Biomed. Microdev. 8 (2006) 255–261.
[42] N. Wiberg, A.F. Holleman, E. Wiberg, Holleman-Wiberg's Inorganic Chemistry, Academic Press, 2001.
[43] S.-W. Yeung, T.M.-H. Lee, H. Cai, I.-M. Hsing, A DNA biochip for on-the-spot multiplexed pathogen identification, Nucleic Acids Res. 34 (2006) e118.
[44] T.B. Christensen, C.M. Pedersen, T.G. Grondahl, T.G. Jensen, A. Sekulovic, D.D. Bang, A. Wolff, PCR biocompatibility of lab-on-a-chip and MEMS materials, J. Micromech. Microeng. 17 (2007) 1527.
[45] N.J. Panaro, X.J. Lou, P. Fortina, L.J. Kricka, P. Wilding, Surface effects on PCR reactions in multichip microfluidic platforms, Biomed. Microdev. 6 (2004) 75–80.
[46] N. Ramalingam, H.-B. Liu, C.-C. Dai, Y. Jiang, H. Wang, Q. Wang, K.M. Hui, H.-Q. Gong, Real-time PCR array chip with capillary-driven sample loading and reactor sealing for point-of-care applications, Biomed. Microdev. 11 (2009) 1007–1020.
[47] W. Wan, J.T.W. Yeow, The effects of gold nanoparticles with different sizes on polymerase chain reaction efficiency, Nanotechnology 20 (2009) 325702.
[48] F. Teng, Y. Guan, W. Zhu, A simple and effective method to overcome the inhibition of Fe to PCR, J. Microbiol. Methods 75 (2008) 362–364.
[49] A. Dahl, M. Sultan, A. Jung, R. Schwartz, M. Lange, M. Steinwand, K.J. Livak, H. Lehrach, L. Nyarsik, Quantitative PCR based expression analysis on a nanoliter scale using polymer nano-well chips, Biomed. Microdev. 9 (2007) 307–314.
[50] L. Gervais, E. Delamarche, Toward one-step point-of-care immunodiagnostics using capillary-driven microfluidics and PDMS substrates, Lab Chip 9 (2009) 3330–3337.
[51] X. Zhou, S. Cai, A. Hong, Q. You, P. Yu, N. Sheng, O. Srivannavit, S. Muranjan, J.M. Rouillard, Y. Xia, X. Zhang, Q. Xiang, R. Ganesh, Q. Zhu, A. Matejko, E. Gulari, X. Gao, Microfluidic PicoArray synthesis of oligodeoxynucleotides and simultaneous assembling of multiple DNA sequences, Nucleic Acids Res. 32 (2004) 5409–5417.
[52] G.V. Kaigala, S. Ho, R. Penterman, C.J. Backhouse, Rapid prototyping of microfluidic devices with a wax printer, Lab Chip 7 (2007) 384–387.
[53] Y. Lu, W. Shi, L. Jiang, J. Qin, B. Lin, Rapid prototyping of paper-based microfluidics with wax for low-cost, portable bioassay, Electrophoresis 30 (2009) 1497–1500.
[54] Y. Lu, W. Shi, J. Qin, B. Lin, Fabrication and characterization of paper-based microfluidics prepared in nitrocellulose membrane by wax printing, Anal. Chem. 82 (2010) 329–335.
[55] W. Wang, Z.X. Li, Y.J. Yang, Z.Y. Guo, Droplet based micro oscillating flow-through PCR chip, in: Micro Electro Mechanical Systems, 2004. 17th IEEE International Conference on MEMS, 2004, pp. 280–283.
[56] A. Gonzalez, R. Grimes, E.J. Walsh, T. Dalton, M. Davies, Interaction of quantitative PCR components with polymeric surfaces, Biomed. Microdev. 9 (2007) 261–266.
[57] D.A. Bruzewicz, M. Reches, G.M. Whitesides, Low-cost printing of poly(dimethylsiloxane) barriers to define microchannels in paper, Anal. Chem. 80 (2008) 3387–3392.
[58] W. Dungchai, O. Chailapakul, C.S. Henry, Electrochemical detection for paper-based microfluidics, Anal. Chem. 81 (2009) 5821–5826.
[59] A.W. Martinez, S.T. Phillips, G.M. Whitesides, Three-dimensional microfluidic devices fabricated in layered paper and tape, Proc. Natl. Acad. Sci. U. S. A. 105 (2008) 19606–19611.
[60] A.W. Martinez, S.T. Phillips, B.J. Wiley, M. Gupta, G.M. Whitesides, FLASH: a rapid method for prototyping paper-based microfluidic devices, Lab Chip 8 (2008) 2146–2150.
[61] Z. Nie, F. Deiss, X. Liu, O. Akbulut, G.M. Whitesides, Integration of paper-based microfluidic devices with commercial electrochemical readers, Lab Chip 10 (2010) 3163–3169.
[63] A. Kunzmann, B. Andersson, T. Thurnherr, H. Krug, A. Scheynius, B. Fadeel, Toxicology of engineered nanomaterials: focus on biocompatibility, biodistribution and biodegradation, Biochim. Biophys. Acta (BBA)-Gen. Subj. 1810 (2011) 361–373.
[64] R. Crameri, R. Kodzius, Z. Konthur, H. Lehrach, K. Blaser, G. Walter, Tapping allergen repertoires by advanced cloning technologies, Int. Arch. Allergy Immunol. 124 (2001) 43–47.
[65] R. Kodzius, C. Rhyner, Z. Konthur, D. Buczek, H. Lehrach, G. Walter, R. Crameri, Rapid identification of allergen-encoding cDNA clones by phage display and high-density arrays, Comb. Chem. High Through. Screen. 6 (2003) 147–154.
[66] R. Kodzius, M. Kojima, H. Nishiyori, M. Nakamura, S. Fukuda, M. Tagami, D. Sasaki, K. Imamura, C. Kai, M. Harbers, Y. Hayashizaki, P. Carninci, CAGE: cap analysis of gene expression, Nat. Methods 3 (2006) 211–222.
[67] T. Shiraki, S. Kondo, S. Katayama, K. Waki, T. Kasukawa, H. Kawaji, R. Kodzius, A. Watahiki, M. Nakamura, T. Arakawa, S. Fukuda, D. Sasaki, A. Podhajska, M. Harbers, J. Kawai, P. Carninci, Y. Hayashizaki, Cap analysis gene expression for high-throughput analysis of transcriptional starting point and identification of promoter usage, Proc. Natl. Acad. Sci. U. S. A. 100 (2003) 15776–15781.

Biographies

Rimantas Kodzius graduated with a PhD degree from the University of Salzburg (Austria, EU) with Prof. Reto Crameri (Swiss Institute of Allergy and Asthma Research, Davos, Switzerland) and Dr. Gerald Walter (Max Planck Institute of Molecular Genetics, Berlin, Germany, EU) in 2002. From 2002 to 2006 he developed and established CAGE (5′-SAGE) technology for large scale high throughput gene promoter mapping at RIKEN institute in Japan. From 2006 to 2009 he worked in the laboratory of Nobel Prize Winner Prof. Sydney Brenner and Prof. Byrappa Venkatesh at the Institute of Molecular and Cell Biology in Singapore on creating libraries for the comparative genomics project on Elephant shark. From 2009 he joined King Abdullah University of Science and Technology (KAUST) and spent one year in Joint Hong Kong University of Science and Technology (HKUST)/KAUST Micro/Nano-Fluidics Laboratory lead by Prof. Weijia Wen. Since 2010 he is working at KAUST in Saudi

Arabia. His research interests are in the area of molecular biology, genomics, transcriptomics, surface chemistry, microfluidic systems and bioMEMS.

Kang Xiao got his BS degree from School of Life Sciences, University of Science and Technology of China (USTC) in 2003. Then he went to HKUST for pursuing PhD in Department of Biology and graduated in 2009. Afterwards, he joined Department of Physics to do postdoctoral research (February–October 2009) under the co-supervision of Prof. Donald Choy Chang (Department of Biology) and Prof. Weijia Wen (Department of Physics). Then he joined marine biology research group under the supervision of Prof. Peiyuan Qian in Department of Biology of HKUST. Dr. Xiao's research interest includes the application of microfluidics into biological research, investigations on mechanisms of apoptosis in mammalian cells, and larval settlement and development.

Jinbo Wu received his BS degree in applied chemistry from Shandong University, Jinan, China, in 2005. He completed his MS degree in materials science and engineering (2007) in HKUST, HongKong. He currently works as a PhD student at HKUST. His research interests include micro/nano fabrication, micro/nano fluidics, biochips.

Xin Yi received his BS degree in physics from the Beijing Normal University, China, 2007. In 2008, he joined the Nano Science and Nano Technology Program, HKUST, Hong Kong and received M.Phil. degree in 2011. His main research areas are microfluidics, LOC (Lab-on-a-Chip), and bioMEMS.

Xiuqing Gong received his MS in analytical chemistry in 2006 from the USTC. Since 2006, he has been a PhD student at HKUST majoring in microfluidics science under the supervision of Prof. Weijia Wen, where he has been doing research on 3D chip fabrication, organic or inorganic material synthesis, drug encapsulation and release, cell culture and evolution, etc. He received his PhD degree in April, 2010 and now continues his postdoctoral research in microfluidic area at Andrew deMello's group (Imperial College, London, UK, EU).

Ian G. Foulds graduated in 2007 with his PhD in electrical engineering from Simon Fraser University, in Burnaby, BC, Canada. He went on to serve in the mechanical engineering department at University of Victoria, as a postdoctoral fellow, until he joined KAUST in 2009 as an assistant professor of electrical engineering, in the division of physical sciences and engineering. His research interests lay in the area of microsystems design and fabrication, with special emphasis on polymer fabrication techniques.

Weijia Wen earned his BS (1982) and MS (1988) degrees at Chongqing University. He completed his PhD (1995) degree in Institute of Physics, Chinese Academy of Science, Beijing. He was a postdoctoral fellow at HKUST (1995–1997) and UCLA (California University at Los Angeles) (1997–1999). He joined HKUST in 1999 and currently is a professor in the Department of Physics, HKUST. Professor Wen's main research interests include soft condensed matter physics, electrorheological (ER) and magnetorheological (MR) fluids, field-induced pattern and structure transitions, micro- and nano-fluidic controlling, microsphere and nanoparticle fabrications, thin film physics, band gap materials, metamaterials and nonlinear optical materials.